Mitigation of inverter-induced noncirculating bearing currents by introducing grounded electrodes into stator slot openings

Vostrov Konstantin, Pyrhönen Juha, Lindh Pia, Niemelä Markku, Ahola Jero

DOI: 10.1109/TIE.2020.3045695

Mitigation of inverter-induced noncirculating bearing currents by introducing grounded electrodes into stator slot openings

K. Vostrov, J. Pyrhönen, *SM, IEEE*, P. Lindh, *SM, IEEE*, M. Niemelä, and J. Ahola

***Abstract*—Modern converter-supplied AC motors are exposed to bearing currents. Despite extensive research and development, the industry still does not have a final solution with acceptable cost and high efficiency. This paper focuses on capacitive bearing currents. After a brief explanation of the phenomenon, an unconventional approach for effective mitigation of the capacitive bearing currents is proposed. The approach suggests using grounded electrodes in the slot openings to reduce the stator-winding-to-rotor-core capacitance and thereby the bearing currents. Different electrode diameters are considered and evaluated by a FEM analysis. The results are verified by laboratory tests. The bearing voltage ratios of the original and modified induction motor are compared.**

***Index Terms*—Ball bearings, electrical discharge machining bearing currents, electrical machines, finite element analysis, induction machines, variable speed drives.**

I. Introduction

Bearing currents are an adverse phenomenon in modern electrical drives. The problem was recognized already in the infancy of electrical motors. The converter era emphasizes the problem, and it remains more or less an open challenge for the industry and researchers. The problem is aggravated by the fact that there are still no standard strategies to fight the bearing currents, and plenty of knowledge related to the problem is not publicly available.

The origins of bearing currents and the current paths inside an electrical machine can be different, but most modern machines suffer from parasitic currents caused by inverter-induced high values of du/dt and common-mode voltage high-frequency components. An industrial electrical machine always has a common magnetic circuit, a multiphase stator winding, a rotor, and, in most cases, ball or roller bearings. As there are conductive parts insulated from each other, an electrical machine can be represented as a set of parasitic capacitances. These capacitances are shown in Fig. 1; they are the stator-winding-to-rotor-core capacitance C_{wr}, the stator-winding-to-stator-core capacitance C_{ws}, the stator-core-to-rotor-core capacitance C_{sr}, and the capacitance of the bearing C_b.

Manuscript received May 14, 2020; revised December 04, 2020; accepted December 04, 2020.

K. Vostrov, J. Pyrhönen, P. Lindh, M. Niemelä, and J. Ahola are with LUT School of Energy Systems, LUT University, PO Box 20, 53851, Lappeenranta, Finland (e-mails: konstantin.vostrov@lut.fi, juha.pyrhonen@lut.fi, pia.lindh@lut.fi, markku.niemela@lut.fi and jero.ahola@lut.fi).

Different types of bearing currents are recognized. Two main groups can be distinguished: circulating (also called inductive or classical) and noncirculating (also called capacitive or electrical discharge machining, EDM) currents. Fig. 1 illustrates the stray current paths for both types of bearing current. In modern machines, the dominating type of bearing current typically depends on the frame size. Smaller machines often suffer from EDM currents and larger from circulating currents, respectively. Among the above-mentioned bearing currents, there are other less significant types of parasitic currents in electrical drive systems: shaft grounding current and stator grounding current, which are reported e.g. in [1]–[3].

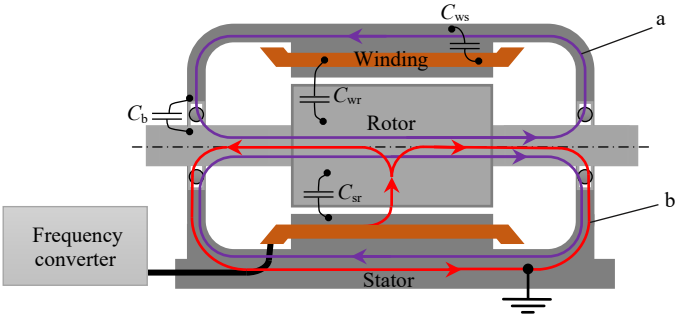

Fig. 1. Schematic of the parasitic capacitances in an electrical machine: stator-winding-to-rotor-core capacitance C_{wr}, stator-winding-to-stator-core capacitance C_{ws}, stator-core-to-rotor-core capacitance C_{sr}, and bearing capacitance C_b. Parasitic current paths: a: circulating, b: noncirculating bearing currents.

A. Circulating bearing currents

Although the circulating bearing currents are not in the scope of this paper, a short description of them is given in the following.

Circulating bearing currents form closed loops within an electrical machine, as indicated by "a" in Fig. 1. The low-frequency circulating currents have been known since the infancy of electrical machines and are mainly caused by an unbalanced magnetic flux, which results from an imperfect motor geometry (which was relevant in early machines), or stator segmentation (relevant in modern large-scale ones). These currents are extensively described in [1], [4], [5].

Another factor contributing to circulating bearing currents is a high common-mode du/dt value, which forces part of the

current to leak from the stator windings through the stator-winding-to-stator-core stray capacitance to the ground [6]. The inductive effect causes high-frequency circulating bearing currents to be generated. Along with low-frequency circulating currents, this mechanism has a considerable contribution in relatively large machines (with a rated power of 75 kW and higher) as described in [4], [7]–[9].

B. Noncirculating bearing currents

1) Overview

A part of the current flowing in the stator winding leaks through the stray capacitance to the stator core and another part to the rotor. The part that leaks to the stator contributes to the circulating bearing currents and usually flows to the machine grounding terminal without causing immediate harm. In contrast, the other part that leaks to the rotor (indicated by "b" in Fig. 1) travels through the bearings on its way to the grounding of the system. This current may cause electrical discharges and is extremely harmful to the ball bearings.

A large proportion of modern AC electrical drives are equipped with a frequency converter, which supplies the motor with higher harmonics, high du/dt values, and common-mode voltage. These features drive the capacitive currents to flow through their parasitic paths. Thus, steel bearings usually suffer from noncirculating bearing currents when a pulse-width-modulated (PWM) voltage-source frequency converter is employed.

An uncommon mitigation method of capacitive currents is studied here. The method is based on modifying the electrical machine by reducing the capacitive coupling between the stator winding and the rotor core. As a result, the bearing voltage ratio (BVR) and thereby bearing currents are reduced.

2) Mitigating techniques available

Various methods have been developed to mitigate bearing currents. Table I lists the state-of-art techniques of reducing capacitive bearing currents.

Techniques aimed to reduce the frequency converter higher voltage harmonics and common-mode voltage are reported extensively in the literature with a wide range of different solutions [10]–[15]. Converter modifications offer significant potential in reducing bearing currents. Such solutions, however, always require to make a choice between an effective but complicated and expensive layout, or less effective but inexpensive software solutions.

It is also possible to suppress the common-mode voltage and higher harmonics on their way from the inverter to the motor by installing a common-mode voltage filter [2], [7], [16]. However, du/dt filters [15]–[19] and common-mode chokes [20]–[22] do not reduce EDM currents.

EDM bearing currents can also be suppressed by introducing machine modifications. For instance, the stray current circuits can be broken partially or completely by minimizing the capacitive couplings [6], [23]–[31] or using ceramic ball bearings [2], [32].

The negative effects of the capacitive currents on the bearings can be reduced if alternative and safe paths for the stray currents are provided. This can be implemented for instance by using conductive grease [33], [34] or shaft grounding devices. Shaft grounding devices form a straightforward and effective countermeasure [35], which has a major drawback: the brushes wear out, they may have contact problems and be sensitive to external conditions, and thus require frequent maintenance. However, various offbeat designs such as microfiber brushes [36], [37] and the use of contactless capacitive shunting [38] can be promising options. Different electrostatic shields reduce capacitive couplings and decrease stray currents.

TABLE I
RANGE OF SOLUTIONS AVAILABLE TO MITIGATE EDM CURRENTS

Technique	Effectiveness*	Drawbacks	Cost
Special modulation strategies [11], [12]	Good: 60% reduction	Limited by the hardware options	Low
New circuit layouts for converters [7]–[9]	Excellent: possible to reach complete elimination	Requires new layout development and adding new components	High
Common-mode voltage filter [2], [7], [16]	Good: 70–100% reduction	Difficulties in the installation may arise	High
Ceramic (hybrid) bearings [2]	Excellent: up to complete elimination	Reduced mechanical load rating, may also require insulated coupling for the connection of a load machine	High
Conductive grease [33]	Average: 50% reduction	Lubrication effectiveness reduced	Mode-rate
Rotor grounding brushes [35], [39]	Good: 80% reduction	Requires service	Low
Electrostatically shielded rotor [23], [31]	Good: reduction of 50–100%	Mounting complexity	High
Brushless grounding device [38]	Good: 80% reduction	Requires significant space for installation; produces extra losses by air friction	Mode-rate
Bearing protection microfiber ring [36]	Good: 50–90% reduction	Must be properly installed; still requires service	Mode-rate

* The percentages given refer to reduction in the EDM current peak amplitude, where 0% means no effect, 100% means complete elimination.

The present paper reviews and verifies the approach of grounded electrodes, discussed in [31]. The approach is aimed at a reduction in PWM-caused EDM bearing currents on the machine side. The proposed design further develops the principle of electrostatic shield applied to reduce capacitive coupling between the rotor core and the stator winding and is not effective against other types of parasitic currents or in cases where, e.g., static electricity can build up and lead to discharges.

The theoretical principles, a FEM-based evaluation, and results obtained from laboratory tests are presented. The results are analyzed and compared with theoretical findings. Finally, the paper is concluded by an evaluation of the feasibility of the approach.

Unlike the previous study [31], the present paper considers an actual electrical machine and verifies the theoretical findings by laboratory experiments. In this paper, a refined FEA is

applied. The paper focuses on practical implementation, describes the system mounting process, and discusses possible issues caused by the system. In addition, possible drawbacks, application notes, limitations, scaling considerations, installation complexity, and costs are addressed.

II. THEORETICAL BACKGROUND

The stator-winding-to-rotor-core capacitance plays an important role in the occurrence of noncirculating bearing currents. A reduction in the capacitance should obviously increase the overall impedance of the stray current circuit, reduce the voltage between the bearing raceways, and prevent bearing lubricant breakdown, which usually leads to EDM current and harmful pitting on bearing raceways.

In the following, the stator-winding-to-rotor-core capacitance C_{wr} will be in the focus of the study, and the method for mitigation of this capacitance is the main contribution of this paper.

Fig. 2 illustrates a simple plate capacitor equivalent circuit of an electrical machine's stator slot. The winding and the rotor surface can be considered electrodes of the capacitor, whereas the winding insulation and the air gap represent the dielectric between these electrodes. This structure offers a path for high-frequency current components. This capacitive coupling is increased by the contribution of the winding overhang. This contribution is taken into account in the calculations.

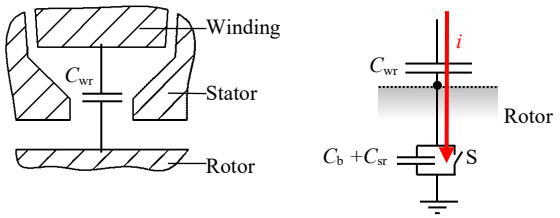

Fig. 2. Left: Stator slot opening and rotor surface. Right: equivalent capacitor circuit. The red arrow indicates the capacitive current path. The rotor connection with the ground terminal is also shown in the circuit. C_b+C_{sr} denotes the capacitance between the bearing raceways when there is no galvanic connection between the rotor and the stator, combined here with the stator-to-rotor capacitance. The switch S indicates the connection that can be formed when the lubricant film breaks down.

As suggested in [31], an effective reduction in the bearing current can be reached by partial electrostatic shielding. Then, capacitive current will bypass the rotor and the bearing. This can be implemented by introducing a grounded electrode in the slot opening, as shown in Fig. 3

The electrode is supposed to act as a partial electrostatic shield. A similar shielding design was proposed in [23] and the approach found a promising countermeasure for EDM current suppression [24]–[27]. The present paper is aimed to further investigate the influence of the shield design options, provide a calculation technique, and contribute to the numerical data related to an industrial electrical machine.

When the electrode is placed into the slot opening or the slot key, the original stator-winding-to-rotor-core capacitance is split into two capacitances in series: the winding-to-electrode C_{we} and the rotor-to-electrode C_{er}. Additionally, because the grounded electrode does not cover all the gaps between the stator teeth, some residual stator-winding-to-rotor-core capacitance C_{wr}' remains as a parallel path, Fig. 3. When using metallic bearings, at certain periods, the rotor has a galvanic connection with the ground. Thus, the rotor side of the equivalent capacitor in Figs. 2 and 3 is grounded. However, if the newly introduced conductor were also grounded (Fig. 3), the capacitive current would not flow through the rotor anymore because a low-impedance bypass is provided. Even though some part of the current may still flow through the remaining C_{wr}', its value would be significantly reduced as C_{wr}' << C_{wr}.

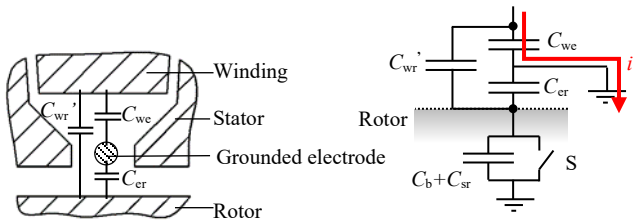

Fig. 3. Left: slot opening of an electrical machine equipped with a grounded electrode. Right: equivalent capacitor representation of the structure. The red arrow indicates the capacitive current path. C_b+C_{sr} denotes the bearing capacitance and the stator-to-rotor capacitance, and the switch S shows the connection that can be formed when the lubricant film breaks down. A fraction of the previously observed capacitance between the rotor and the winding remains as C_{wr}', where C_{wr}'<< C_{wr}.

The electrodes are introduced in all stator slot openings and connected to the ground terminal at one end. Connecting the electrodes at only one end prevents the formation of closed loops, which could result in the appearance of a squirrel cage effect and extra eddy current losses [31], [40]. Fig. 4 shows a machine stator equipped with grounded electrodes. Different designs and positions of the electrode system were presented in [31]. In this study, however, the simplest option with a single-wire electrode was chosen for a detailed analysis and empirical verification of the method.

A common parameter to evaluate the potential risk of bearing currents is the bearing voltage ratio (BVR). Together with the supply voltage, the voltage across the bearing can be determined with the BVR known. The BVR is the ratio between the bearing voltage U_b and the common-mode voltage at the motor terminals U_{cm}. BVR can be defined with the machine capacitances [2], [41]:

$$BVR = \frac{U_b}{U_{cm}} = \frac{C_{wr}}{C_{wr} + C_{sr} + 2C_b} \quad (1)$$

where U_b is the voltage between the shaft and the grounding, U_{cm} is the common-mode voltage, and C_{wr}, C_{sr}, and C_b are the stator-winding-to-rotor-core, stator-core-to-rotor-core, and bearing capacitance respectively.

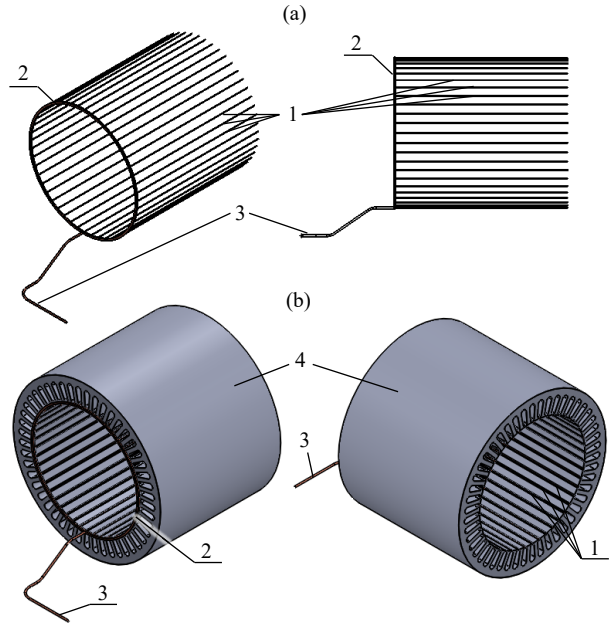

Fig. 4. Concept of grounded electrodes mounted in slots; a) grounded electrode and b) stator stack with electrodes installed. The electrodes can be joined either by a ring at the stack end and grounded together or separately. 1: electrodes, 2: common collecting conductor (ring), 3: wire to the network PE terminal, and 4: stator.

(1) can be explained by using the equivalent circuit of the machine capacitances shown in Fig. 5, left [2], [37]. The figure demonstrates that the parasitic capacitances form a capacitive voltage divider. A share of the high-frequency common-mode voltage is observed over the bearing as the bearing voltage U_b.

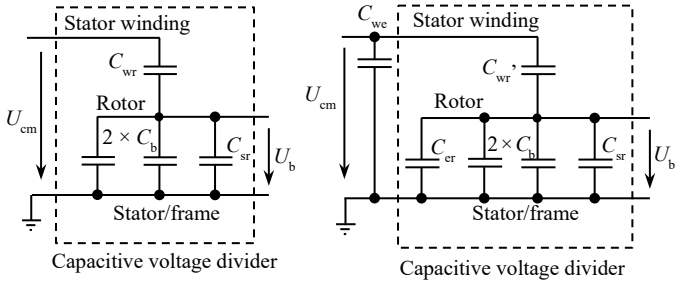

Fig. 5. Equivalent circuit of the main capacitances of an AC motor: left – regular AC motor, right – the motor equipped with stator grounded electrodes. The elements making up the capacitive voltage divider are highlighted in both circuits.

When grounded electrodes are applied, the equivalent circuit must be changed accordingly. The electrodes cause the stator-winding-to-rotor-core capacitance C_{wr} of the regular machine (Fig. 2) to be replaced with the series-connected capacitances C_{we} and C_{er} and the parallel residue capacitance C_{wr}' (Fig. 3). The equivalent circuit of the modified machine is shown on the right in Fig. 5. When defining the BVR based on the capacitive voltage divider principle, the equation for the modified machine is written as

$$BVR = \frac{U_b}{U_{cm}} = \frac{C_{wr}'}{C_{wr}' + C_{sr} + 2C_b + C_{er}} \quad (2)$$

where C_{wr}' is the residual stator-winding-to-rotor-core capacitance and C_{er} is the capacitance between the rotor core and the electrode introduced in the slot opening. The term C_{we} is not presented in the BVR equation because this capacitance stays in parallel with the voltage divider and does not affect the ratio.

In theory, the BVR is defined with the machine capacitances. In practice, the capacitances cannot be directly measured. The problem in measurements is that in a real machine there is always extra stator-to-frame capacitance C_{sf} in parallel, which cannot be eliminated. It is, e.g., ~10 nF with 15 kW machines, while C_{wr} is only 100–200 pF (1–2% of C_{sf}). The limited accuracy of LCR meters and uncertainties in measurements make the practical measurement of C_{wr} difficult. However, the machine stray capacitances can be found according to the circuit relationship as described in [42]. Alternatively, the BVR can be defined as a ratio of the bearing voltage to the common-mode voltage [41], [43]. Both methods were utilized in the present work.

III. Experimental Evaluation

The quantitative evaluation of the proposed approach was performed by a study of a 15 kW 4-pole 36-slot ABB M3BP160 MLB4-series induction motor.

A. FEM-based evaluation of the method

Preliminary results were obtained by a finite element analysis, performed in the FEMM v.4.2 software. The modeling approach introduced in [31] was applied. The slot dimensions used in the computation are shown in Fig. 6. The lamination stack length is 272 mm.

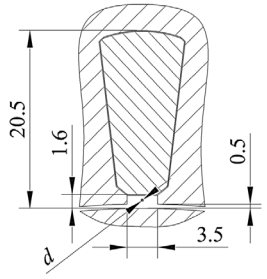

Fig. 6. Dimensions of the 15 kW 4-pole 36-slot machine under study [in mm]. d is the varying diameter of the grounded electrode.

In the study, the capacitances C_{wr} and C_{sr} were estimated for an unmodified machine and for a machine equipped with slot electrodes. The capacitances calculated for the whole machine and the BVRs obtained are collected in Table II. The BVRs were calculated using (1) for the original machine and (2) for the machine with grounded electrodes. In the BVR calculation, the ceramic bearing capacitance C_b was measured to be 27 pF.

The 2D FEM results only correspond to the lamination stack region and ignore the contribution of the end windings. According to [44], in 15 kW machines, the proportion of the end winding is about 40% of the total stator-winding-to-rotor-core capacitance. Therefore, the end winding capacitance $C_{wr,ew}$ can be found from the core-area capacitance $C_{wr,core}$ of the original machine multiplied by a factor of 40/60, resulting in $C_{wr,ew}$ = 84pF.

In Table II, the 2D FEM-calculated capacitances that do not take the end-winding region into account are indicated by the subscript "core", $C_{wr,core}$. The updated stator-winding-to-rotor-core capacitance in which the lamination stack and the end-winding regions are considered is denoted by C_{wr} in Table II and later on in the paper. The stator-core-to-rotor-core capacitance is not affected by the end windings, and therefore, there is no need for a similar correction in C_{sr}. The data are analyzed further in the Discussion section.

TABLE II
ESTIMATED STRAY CAPACITANCES AND BVRS FOR REGULAR MOTORS AND MOTORS MODIFIED WITH ELECTRODES OF DIFFERENT DIAMETERS

Motor type	$C_{wr,core}$, [pF]	C_{wr}, [pF]	C_{sr}, [nF]	C_{er}, [pF]	BVR, [%]
Regular motor; no grounded electrodes	126	210*	2.61	–	7.32
Modified motor; grounded electrodes applied. Electrode diameters:					
0.1 mm	88.1	172*'	2.61	229.6	5.63
0.3 mm	69.5	154*'	2.60	364.8	4.84
0.5 mm	55.6	140*'	2.60	495.3	4.25
0.75 mm	41.8	126*'	2.59	680.0	3.64
1.0 mm	30.2	114*'	2.59	912.5	3.11

Values indicated by * are found as $C_{wr,core} + C_{wr,ew}$.
Values indicated by ' correspond to C_{wr}' of Fig. 3.

B. Verification with a real electrical machine

A study on a real machine was carried out in the laboratory. First, the BVR of the 15 kW motor equipped with ceramic ball bearings was measured. Then, the motor was equipped with enamelled copper wire slot electrodes with a diameter of 0.3 mm. The electrodes were placed on the slot insulation along the lamination stack length. They did not cover the end-winding region. The electrodes were fixed in the middle of the slot openings. In serial manufacturing, introducing electrodes into slot keys would be reasonable. At the drive end of the core, the electrodes were only cut making sure that they did not have any galvanic contact to the stator core. At the non-drive end, the electrodes were connected to the ground terminal. Fig. 7 shows the slots and a general view of the modified machine.

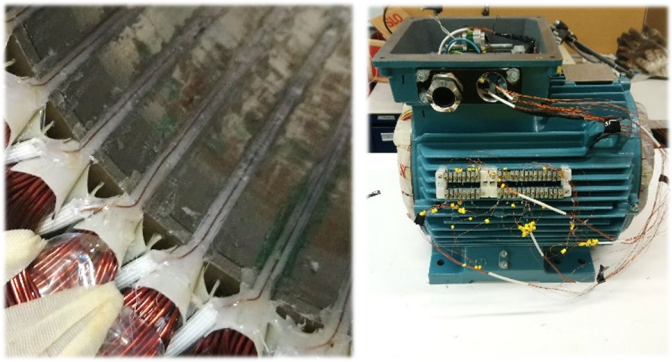

Fig. 7. Left: the stator slots with grounded electrodes added. Right: a general view of the modified machine. 36 wires coming from the stator slots are collected at an external terminal block.

1) Verification with machine capacitances measured

In a similar way as it was done in the theoretical stage, the BVRs were found for both the original and modified machines using the actual values of the capacitances employed in (1) and (2). As was mentioned above, straightforward measurement of the machine stray capacitances is not possible, and the technique presented in [42] was repeated in this work to establish the desired values. The initial measurements were peformed with disconnected motors at a standstill state using an Agilent U1733C RLC measuring device and a measurement frequency of 1 kHz. The measurement results were further processed using the formulas proposed in [42].

The capacitances of C_{wr} and C_{sr}, which have to be known for the BVR calculation of the original machine (1), were found by using the algorithm and equations given in [42].

The equation of the BVR for the modified machine (2) has an extra term of C_{er}. The process of finding the values of C_{er} and C_{sr} in such a machine requires development of a new calculation approach. However, in Fig. 5 (right), the capacitances C_{sr} and C_{er} are connected in parallel, and thus, the equation numbered (8) in [42] can be used to determine the total value of $C_{sr} + C_{er}$.

The bearing capacitance was measured to be $C_b = 27$pF. The results are presented in Table III.

TABLE III
MEASURED STRAY CAPACITANCES AND BVRS FOR A REGULAR MOTOR AND A MOTOR MODIFIED WITH GROUNDED ELECTRODES

Motor type	C_{wr} or C_{wr}', [pF]	C_{sr}, [nF]	$C_{sr} + C_{er}$, [nF]	BVR, [%]
Regular motor; no grounded electrodes	180.7	2.08	–	7.8
Modified motor; grounded electrodes with a diameter of 0.3 mm are applied.	63.3*	–	2.25	2.7

Value indicated by * is correspond to C_{wr}' of Fig. 3.

2) Verification with the bearing voltage to the common-mode voltage ratio

In the no-load test, when the machine was supplied by an ABB ACS400 frequency converter, the bearing voltage ratio was defined as U_b / U_{cm} using (1) or (2). Because of the stator delta connection, an artificial star for measuring U_{cm} was formed with three 10 MΩ resistors. To facilitate shaft voltage measurement, ceramic ball bearings were used. U_b and U_{cm} were measured with Rohde&Schwarz RT-ZD01 differential probes. The laboratory setup is illustrated in Figs. 8 and 9.

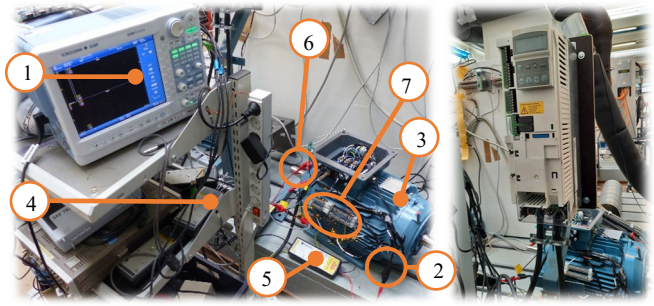

Fig. 8. Left: laboratory setup; 1: multichannel oscilloscope Yokogawa DL850, 2: artificial neutral point connection, 3: motor under test, 4: Rohde&Schwarz RT-ZD01 differential probe for the shaft voltage measurement, 5: Rohde&Schwarz RT-ZD01 differential probe for the common-mode voltage measurement, 6: brush connection to the shaft, and 7: slot electrodes collected at the external terminal block, connected to the frame and further to the ground terminal of the system. Right: ABB ACS400 frequency converter was used to supply both the original and the modified motor.

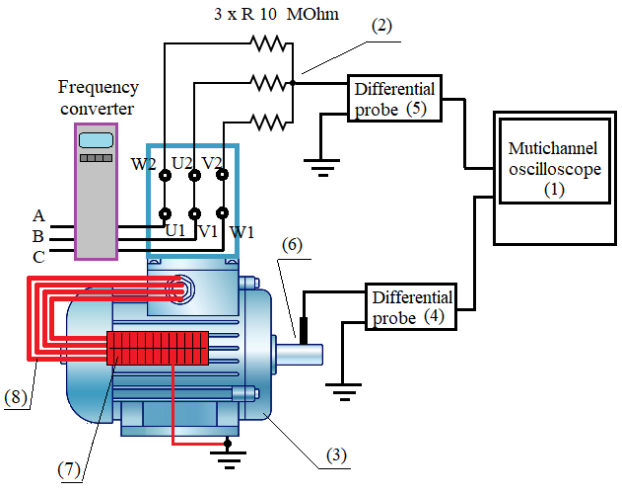

Fig 9. Laboratory setup; 1: Yokogawa DL850, 2: artificial neutral point connection, 3: motor, 4: differential probe for U_b, 5: differential probe for U_{cm}, 6: brush connection, 7: electrode terminal box, 8: 36 electrodes. The parts indicated by red show the elements added to the modified motor.

Fundamental frequencies of 10, 20, 30, and 40 Hz were used. Examples of the shaft voltage waveforms taken from the original and modified machines at the 20 Hz supply frequency are shown in Fig. 10. Examples of the common-mode voltage waveforms for both motors are shown in Fig. 11. The waveforms taken for 10, 30, and 40 Hz fundamental frequencies are almost identical to the ones shown for 20 Hz.

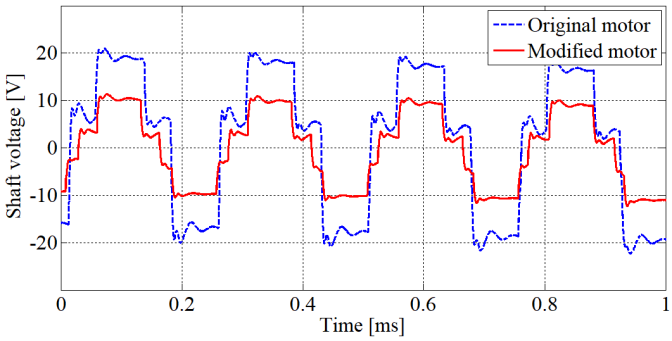

Fig. 10. Measured shaft voltage at the 20 Hz fundamental PWM supply for the regular and modified 15 kW induction motors.

The shaft voltage measured from the modified motor has a notably lower amplitude than in the regular motor. The amplitude of the common-mode voltage, as seen in Fig. 11, remains at the same level for both motors.

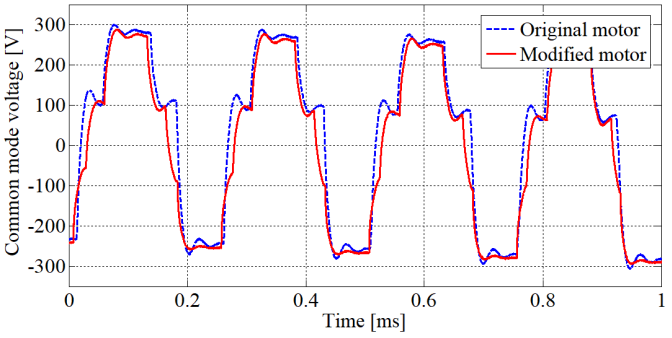

Fig. 11. Measured common-mode voltage at 20 Hz for the regular and modified 15 kW induction motors.

U_b and U_{cm} peak values were used in the analysis. The measured BVRs and the obtained average BVR value are shown in Table IV. On average, a 44% reduction in the BVR was achieved with this simple test approach.

TABLE IV
MEASURED RAW DATA

Supply frequency, [Hz]	BVR [%], peak-to-peak	
	Regular machine	Modified machine
10	7.13	3.97
20	7.15	3.98
30	7.13	3.92
40	7.05	3.93
Average value	7.1	3.95

IV. DISCUSSION

Fig. 12 shows FEA results for both the BVR and $C_{wr}/C_{wr,nom}$ as a function of electrode diameter. $C_{wr,nom}$ is the stator-winding-to-rotor-core capacitance of the unmodified motor.

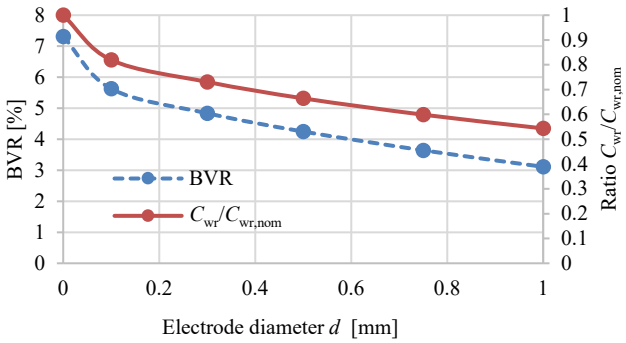

Fig. 12. BVR and $C_{wr}/C_{wr,nom}$ as a function of the diameter of the grounded electrode placed on the slot key. $d = 0$ corresponds to the original motor.

Introducing even a thin grounded electrode gives a significant reduction in C_{wr} and a corresponding reduction in the BVR. According to Fig. 12, when 0.1 mm electrodes are mounted on the slot keys, the BVR decreases by almost 25% (from BVR = 7.32% to BVR = 5.63%). A further increase in the electrode diameter reduces the BVR more, but less dramatically.

In the laboratory tests, the machine was equipped with 0.3 mm slot-key-surface electrodes. The measurement results, given in Tables III and IV, show a decreasing BVR trend and are in line with theory. Fig. 13 compares the experimentally obtained BVRs with the values given by the 2D FEM-based approach.

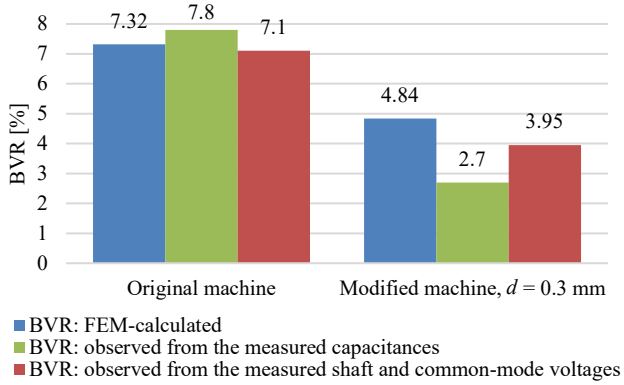

Fig. 13. BVR computed and measured for the original and modified motor with 0.3 mm electrodes on the slot keys.

In the case of an electrode diameter of 0.3 mm, the difference between the calculated and measured BVRs was 44% when the measured capacitances were used and 18% when the BVR was obtained by using the common-mode and shaft voltage amplitudes. The analytical calculations underestimated the effect. The main reasons that may cause an error in the calculation results are:

1) Inaccurate motor geometry; it was measured by the authors. A ±0.5 mm error in dimensions is possible.

2) Simplified representation of the winding: the winding was modeled as a solid piece of copper instead of thin copper wires.

3) Share of the end winding, which is taken as 40%, is a rough estimation and can vary depending on the design.

4) In the FEM calculations, meshing and numerical issues may also contribute to the error.

Furthermore, when the capacitance measurement was performed, the limited accuracy of the RLC meter and the measurement issues mentioned at the end of Section II also contribute to the error. Based on that, the BVR measurement performed as a ratio of shaft-to-common voltages is preferable in practical cases.

However, the results have an acceptable accuracy and a matching trend. The behavior of the BVR and C_{wr}, caused by the varying electrode diameter shown in Fig. 12 obtained by an analytical approach, can be considered verified in practice. The calculation method can be applied in similar studies.

As stated in [3], [45], the bearing EDM threshold voltage is usually 10–30 V, and can be only 5 V in the smallest machines [46]. The bearing voltage peak value of the tested 15 kW machine modified with the 0.3 mm diameter wire had $U_b = 10$ V and can be considered relatively safe.

Different designs of electrostatic shields tested by different authors on the machines in the range of 3–37 kW [23]–[26] give a bearing voltage reduction of 50–70%. In our test bench, a reduction in U_b from the peak value of 20 V to 10 V, i.e., a 50% reduction, was obtained. With the change in the wire diameter, this number is expected to vary together with the BVR as shown in Fig. 12, i.e., with a growing wire diameter, the effectiveness of U_b reduction should also increase.

Applying the presented approach to frequency-converter-supplied electrical machines could increase the overall reliability of the system by a significant reduction in the noncirculating bearing currents. Even though the introduction of complicated structures (as in [31]) or extra wedges (as in [30]) into the slot opening definitely require special tools and skills, introducing only one thin electrode seems efficient and can be considered a possible practical modification in electrical machines. The installation of grounded electrodes requires minimum space in an electrical machine and in most cases, regardless of the machine size, it can be implemented in the existing winding position while the slot copper space factor remains unchanged. In the test machine presented in this paper, the electrode with a diameter of 0.3 mm was successfully placed in the existing 1 × 3.5 mm slot opening. The simplicity and low cost of the machine modification are among the advantages of the proposed approach.

The approach presented here has about the same bearing current reduction potential as the approach of introducing extra wedge insulation presented in [30]. A FEM-based computation, conducted for both approaches with the same machine geometry, gives almost equal BVR reduction indicators. During verification with an actual machine, it turned out that the modification proposed in the present paper reduces the shaft voltage amplitude to the same level as the application of thicker wedges. Taking this into account, the choice between the proposed method or countermeasures suggested in [30] should mainly be made on the basis of considerations other than the degree of reduction in the BVR.

The approach is highly applicable to machines of different power ratings. With different machine sizes, the size of the slot opening varies accordingly. In larger machines, several thin wires can be integrated into the slot key to achieve a significant reduction in the BVR. To keep the desired BVR reduction rate in machines of different sizes, the diameter and number of wires in one slot opening should be adjusted individually in each case.

As suggested in [23], the utilization of electrostatic shields, which affect both the core area and the end windings, provides an opportunity to reduce the bearing voltage by 100%. Special end windings shields, such as [47], used in parallel with the method presented here, are expected to give the maximum possible bearing voltage reduction.

In large scale motors—with a shaft height larger than 280 mm (over 100 kW)—the suggested countermeasure should not be considered the main method because according to the literature, EDM bearing currents are not dominant compared with circulating bearing currents in high-power inverter motors.

One drawback of the proposed method is a possible minor increase in the circulating bearing currents as the occurrence of capacitive current from the winding to the slot key electrode is easier. However, C_{wr} is much smaller than C_{ws}, and thus, its contribution to the circulating bearing currents is also negligibly small.

Another concern is that, in principle, electrode eddy currents can produce some extra losses. To minimize losses, the thinnest possible wire or a set of parallel insulated wires should be used [6].

Because copper wires have magnetic permeability close to unity, and because the magnetic flux is mainly concentrated in the stator teeth [24], the proposed mitigation method for bearing currents would not cause any negative effect on the magnetic circuit and torque production characteristics of the machine.

Finally, a proper ground connection of the electrodes on the slots must be maintained. Using the modified machine with nongrounded slot electrodes would have a negative effect, which slightly increases the BVR. In the example case of the 15 kW machine, the BVR increased from 7.1 to 7.3% with disconnected electrodes.

V. Conclusion

A method for suppressing noncirculating bearing currents, based on reducing the winding-to-rotor capacitance by installing grounded electrodes on slot keys, was studied. Based on 2D-FEM computations, it was shown with a 15 kW industrial motor that installing only one thin grounded electrode on the slot key effectively reduces the stator-winding-to-rotor-core capacitance responsible for the noncirculating bearing currents. Increasing the electrode diameter results in a minor additional reduction in the BVR.

A four-pole 15 kW industrial induction motor was modified and tested. The practical results are in line with the computed values. Based on both a theoretical analysis and laboratory tests, it can be concluded that introducing grounded electrodes is an effective countermeasure against capacitive bearing currents.

Even though the presented countermeasure can already be employed as a ready-to-use solution, the full potential of the approach has not yet been reached. The field reports and long-time running test results of the drive systems equipped with the proposed shielding system are of great interest.

Further studies into bearing current suppression techniques that work on the electrostatic shielding principle would be required to design a shielding system capable of reducing also capacitive coupling caused by the end-winding region. Finally, the question of the effectiveness and feasibility of the use of several different bearing current suppression techniques at a time is an open question and should be investigated in the future work.

VI. REFERENCES

[1] J. Pyrhönen, V. Hrabovcova, and R. Scott Semken, Electrical Machine Drives Control: An Introduction, John Wiley & Sons Ltd, ch. 13, 2016.

[2] A. Muetze, "Bearing Currents in Inverter-Fed AC-Motors," Ph.D. dissertation, Dept. of Electrical and Computer Engineering, Technical Univ. of Darmstadt, Darmstadt, Germany, 2004.

[3] T. Plazenet, T. Boileau, C. Caironi, and B. Nahid-Mobarakeh, "A Comprehensive Study on Shaft Voltages and Bearing Currents in Rotating Machines," in IEEE Transactions on Industry Applications, vol. 54, no. 4, pp. 3749-3759, July-Aug. 2018.

[4] A. Muetze and A. Binder, "Calculation of Circulating Bearing Currents in Machines of Inverter-Based Drive Systems," in IEEE Transactions on Industrial Electronics, vol. 54, no. 2, pp. 932-938, April 2007.

[5] S. Chen, T. A. Lipo, and D. W. Novotny, "Circulating Type Motor Bearing Current in Inverter Drives," Industry Applications Magazine, Vol. 4, No. 1, pp. 32–38, 1998.

[6] P. Maki-Ontto and J. Luomi, "Bearing current prevention of converter-fed AC machines with a conductive shielding in stator slots," IEEE International Electric Machines and Drives Conference, 2003 (IEMDC'03), Madison, WI, USA, 2003, vol.1, pp. 274-278.

[7] Variable Speed Drives & Motors. Motor Shaft Voltages and Bearing Currents Under PWM Inverter Operation. Technical Report No. 2. 2nd edition. 2006. GAMBICA / REMA.

[8] A. Muetze, V. Niskanen, and J. Ahola, "On Radio-Frequency-Based Detection of High-Frequency Circulating Bearing Current Flow," in IEEE Transactions on Industry Applications, vol. 50, no. 4, pp. 2592-2601, July-Aug. 2014.

[9] AEGIS, "What Is the Effect of PWM Drives on Electric Motor Bearings?," 21 February 2018. [Online]. Available: https://est-aegis.info/tag/common-mode-voltage/. [Accessed 20 September 2020].

[10] R. K. Dhatrak, R. K. Nema, S. K. Dash, and D. M. Deshpande, "Mitigation of bearing current and shaft voltage using five level inverter in three phase induction motor drive with SPWM technique," 2015 International Conference on, Industrial Instrumentation and Control (ICIC), Pune, 2015, pp. 1184-1189.

[11] D. Han, C. T. Morris, and B. Sarlioglu, "Common-Mode Voltage Cancellation in PWM Motor Drives With Balanced Inverter Topology," in IEEE Transactions on Industrial Electronics, vol. 64, no. 4, pp. 2683-2688, April 2017.

[12] C. T. Morris, D. Han, and B. Sarlioglu, "Reduction of Common Mode Voltage and Conducted EMI Through Three-Phase Inverter Topology," in IEEE Transactions on Power Electronics, vol. 32, no. 3, pp. 1720-1724, March 2017.

[13] H. Chen and H. Zhao, "Review on pulse-width modulation strategies for common-mode voltage reduction in three-phase voltage-source inverters," in IET Power Electronics, vol. 9, no. 14, pp. 2611-2620, 16 Nov. 2016.

[14] A. M. Hava and E. Ün, "A High-Performance PWM Algorithm for Common-Mode Voltage Reduction in Three-Phase Voltage Source Inverters," in IEEE Transactions on Power Electronics, vol. 26, no. 7, pp. 1998-2008, July 2011.

[15] R. M. Tallam, R. J. Kerkman, D. Leggate, and R. A. Lukaszewski, "Common-Mode Voltage Reduction PWM Algorithm for AC Drives," in IEEE Transactions on Industry Applications, vol. 46, no. 5, pp. 1959-1969, Sept.-Oct. 2010.

[16] A. K. Ryszard Strzelecki, R. Smolenski, "Reduction of the bearing current in PWM motor drives by means of common mode voltage cancellation," in Power Quality and Utilization - EPQU'01: 6th International Conference, Cracow 2001, Poland, 2001, pp. 439-444.

[17] J. P. Ström, J. Tyster, J. Korhonen, M. Purhonen, and P. Silventoinen, "Active du/dt filter dimensioning in variable speed AC drives," Proceedings of the 2011 14th European Conference on Power Electronics and Applications, Birmingham, 2011, pp. 1-7.

[18] W. Wu, Y. Jiang, Y. Liu, M. Huang, Y. He, and S.-H. Chung, "A new passive filter design method for overvoltage suppression and bearing currents mitigation in a long cable based PWM inverter-fed motor drive system," 2016 IEEE 8th International Power Electronics and Motion Control Conference (IPEMC-ECCE Asia), Hefei, 2016, pp. 3103-3110.

[19] J. Kalaiselvi and S. Srinivas, "Passive common mode filter for reducing shaft voltage, ground current, bearing current in dual two level inverter fed open end winding induction motor," 2014 International Conference on Optimization of Electrical and Electronic Equipment (OPTIM), Bran, 2014, pp. 595-600.

[20] N. Zhu, J. Kang, D. Xu, B. Wu, and Y. Xiao, "An Integrated AC Choke Design for Common-Mode Current Suppression in Neutral-Connected Power Converter Systems," in IEEE Transactions on Power Electronics, vol. 27, no. 3, pp. 1228-1236, March 2012.

[21] A. Muetze, "Scaling Issues for Common-Mode Chokes to Mitigate Ground Currents in Inverter-Based Drive Systems," in IEEE Transactions on Industry Applications, vol. 45, no. 1, pp. 286-294, Jan.-feb. 2009.

[22] H.W.Oh, "Common Mode Chokes or Cores (CMCs) Cannot Prevent Bearing Failure in All Motors," Motor and Drive Systems Conference, January 2017, Orlando, Florida.

[23] D. F. Busse, J. M. Erdman, R. J. Kerkman, D. W. Schlegel, and G. L. Skibinski, "An evaluation of the electrostatic shielded induction motor: a solution for rotor shaft voltage buildup and bearing current," in IEEE Transactions on Industry Applications, vol. 33, no. 6, pp. 1563-1570, Nov.-Dec. 1997.

[24] F. J. T. E. Ferreira, M. V. Cistelecan, and A. T. de Almeida, "Evaluation of Slot-Embedded Partial Electrostatic Shield for High-Frequency Bearing Current Mitigation in Inverter-Fed Induction Motors," in IEEE Transactions on Energy Conversion, vol. 27, no. 2, pp. 382-390, June 2012.

[25] J. Quan, B. Bai, Y. Wang, and W. Liu, "Research on electrostatic shield for discharge bearing currents suppression in variable-frequency motors," 2014 17th International Conference on Electrical Machines and Systems (ICEMS), Hangzhou, 2014, pp. 139-143.

[26] S. Gerber and R. Wangi, "Reduction of Inverter-Induced Shaft Voltages Using Electrostatic Shielding," 2019 Southern African Universities Power Engineering Conference/Robotics and Mechatronics/Pattern Recognition Association of South Africa, (SAUPEC/RobMech/PRASA), Bloemfontein, South Africa, 2019, pp. 310-315.

[27] B. Heidler, K. Brune, and M. Doppelbauer, "Design aspects of an electrostatic shield in an electric machine for hybrid electric vehicles," 8th IET International Conference on Power Electronics, Machines and Drives (PEMD 2016), Glasgow, 2016, pp. 1-6.

[28] J. Park, T. R. Wellawatta, S. Choi, and J. Hur, "Mitigation Method of the Shaft Voltage According to Parasitic Capacitance of the PMSM," in IEEE Transactions on Industry Applications, vol. 53, no. 5, pp. 4441-4449, Sept.-Oct. 2017.

[29] A slot-wedge of an electric machine, by J. Pyrhönen, (2018, Nov. 22). WO2018211174. Accessed on: May. 13, 2020. [Online]. Available: https://patentscope.wipo.int/search/en/detail.jsf?docId=WO2018211174

[30] K. Vostrov, J. Pyrhönen, M. Niemelä, J. Ahola, and P. Lindh, "Mitigating noncirculating bearing currents by a correct stator magnetic circuit and winding design," in IEEE Transactions on Industrial Electronics, paper 19-TIE-4243

[31] K. Vostrov, J. Pyrhönen, J. Ahola, and M. Niemelä, "Non-circulating Bearing Currents Mitigation Approach Based on Machine Stator Design Options," 2018 XIII International Conference on Electrical Machines (ICEM), Alexandroupoli, 2018, pp. 866-872.

[32] J. A. Oliver, G. Guerrero, and J. Goldman, "Ceramic Bearings for Electric Motors: Eliminating Damage with New Materials," in IEEE Industry Applications Magazine, vol. 23, no. 6, pp. 14-20, Nov.-Dec. 2017.

[33] A. Gonda, R. Capan, D. Bechev, and B. Sauer, "The Influence of Lubricant Conductivity on Bearing Currents in the Case of Rolling Bearing Greases," in Lubricants, vol. 7, issue 12, article number 108, Dec. 2019.

[34] J. Suzumura, "Prevention of Electrical Pitting on Rolling Bearings by Electrically Conductive Grease," Quarterly Report of RTRI, vol. 57, no. 1, pp. 42-47, 2016.

[35] T. Bishop, "Dealing with shaft and bearing currents," Kentucky Service Co., 2017. [Online]. Available: http://www.kyservice.com/wp-content/uploads/2017/03/EASA-Shaft-Bearing-Currents.pdf. [Accessed 20 September 2020].

[36] A. Muetze and H. W. Oh, "Design Aspects of Conductive Microfiber Rings for Shaft-Grounding Purposes," in IEEE Transactions on Industry Applications, vol. 44, no. 6, pp. 1749-1757, Nov.-dec. 2008.

[37] A. Muetze and H. W. Oh, "Application of Static Charge Dissipation to Mitigate Electric Discharge Bearing Currents," in IEEE Transactions on Industry Applications, vol. 44, no. 1, pp. 135-143, Jan.-feb. 2008.

[38] D. C. Ludois and J. K. Reed, "Brushless Mitigation of Bearing Currents in Electric Machines Via Capacitively Coupled Shunting," in IEEE Transactions on Industry Applications, vol. 51, no. 5, pp. 3783-3790, Sept.-Oct. 2015.

[39] S. Bell, T. J. Cookson, S. A. Cope, R. A. Epperly, A. Fischer, D. W. Schlegel, and G. L. Skibinski, "Experience with variable-frequency drives and motor bearing reliability," in IEEE Transactions on Industry Applications, 37(5), pp. 1438–1446, 2001.

[40] Dynamoelectric machines with shaft voltage prevention method and structure, by David B. Hyypio, (1998, Oct. 13). US patent 5 821 652 A.

[41] A. Muetze and A. Binder, "Calculation of Motor Capacitances for Prediction of the Voltage Across the Bearings in Machines of Inverter-Based Drive Systems," IEEE Transactions on Industry Applications, vol. 43, no. 3, pp. 665-672, May-june 2007.

[42] X. Ma, R. Liu, B. Zheng, and Y. Zhang, "Analysis and calculation of capacitance parameters in induction machines to predict shaft voltage," 2012 15th International Conference on Electrical Machines and Systems (ICEMS), Sapporo, 2012, pp. 1-5.

[43] V. Särkimäki, "Radio Frequency Measurement Method for Detecting Bearing Currents in Induction Motors," Ph.D. dissertation, Dept. LUT Energy, Lappeenranta University of Technology, Lappeentanta, Finland, 2009.

[44] K. Vostrov, J. Pyrhönen, and J. Ahola, "The Role of End-Winding in Building Up Parasitic Capacitances in Induction Motors," 2019 IEEE International Electric Machines & Drives Conference (IEMDC), San Diego, CA, USA, 2019, pp. 154-159.

[45] D. Busse, J. Erdman, R. J. Kerkman, D. Schlegel, and G. Skibinski, "Bearing currents and their relationship to PWM drives," in IEEE Transactions on Power Electronics, vol. 12, no. 2, pp. 243-252, March 1997.

[46] O. Magdun, Y. Gemeinder, and A. Binder, "Prevention of harmful EDM currents in inverter-fed AC machines by use of electrostatic shields in the stator winding overhang," IECON 2010 - 36th Annual Conference on IEEE Industrial Electronics Society, Glendale, AZ, 2010, pp. 962-967.

[47] K. Vostrov, J. Pyrhönen, and J. Ahola, "Shielding the end windings to reduce bearing currents," 2020 International Conference on Electrical Machines (ICEM), Gothenburg, 2020, pp. 1431-1437

Konstantin Vostrov was born in Leningrad, Russia, in 1991. He received the B.Sc. degree in the field of Electrical Engineering, Electromechanics and Electrotechnology from Peter the Great St. Petersburg Polytechnic University in 2014, and the double-degree M.Sc. from the Peter the Great St. Petersburg Polytechnic University in 2015 and Lappeenranta University of Technology in 2016. He is currently a doctoral student at Lappeenranta–Lahti University of Technology LUT, and his major research interest at the current time is the investigation of the bearing current phenomena in electrical drives and development of the appropriate countermeasures.

Juha Pyrhönen (M'06), was born in 1957 in Kuusankoski, Finland, received the Doctor of Science (D.Sc.) degree in Electrical Engineering from Lappeenranta University of Technology (LUT), Finland in 1991. He became an Associate Professor of Electrical Engineering at LUT in 1993 and a Professor of Electrical Machines and Drives in 1997. He is engaged in research and development of electric motors and electric drives. His current interests include different synchronous machines and drives, induction motors and drives, and solid-rotor high-speed induction machines and drives.

Pia Lindh (M'04) born in Helsinki in 1969, received her M.Sc. degree in energy technology in 1998 and her D.Sc. degree in electrical engineering (Technology) in 2004 from Lappeenranta University of Technology (LUT), Lappeenranta, Finland. She is currently serving as an associate professor at the Department of Electrical Engineering in LUT Energy, Lappeenranta, where she is engaged in teaching and research of electric motors and electric drives.

Markku Niemelä received the B.Sc. degree in electrical engineering from Helsinki Institute of Technology, Helsinki, Finland, in 1990 and the M.Sc. and D.Sc. degrees in technology from Lappeenranta University of Technology (LUT), Lappeenranta, Finland, in 1995 and 1999, respectively. He is currently a Senior Researcher with the Carelian Drives and Motor Centre, LUT. His current interests include motion control, control of line converters, and energy efficiency of electric drives.

Jero Ahola was born in Lappeenranta, Finland, in 1974. He received the M.Sc. and D.Sc. degrees in electrical engineering from Lappeenranta University of Technology (LUT), Lappeenranta, Finland, in 1999 and 2003, respectively. He is currently Professor of Energy Efficiency in Electrically Driven Systems with the Department of Electrical Engineering, LUT. His research interests include energy efficiency in electrical-motor-driven systems, solar photovoltaic systems, water electrolysis, power-to-X processes, and power-line communication in the motor cables of variable speed electric drives.